RSC Advances

ROYAL SOCIETY OF CHEMISTRY

www.rsc.org/advances

Parameters affecting Carbon Nanofibers Electrode for Measurement of Cathodic Current in Electrochemical Sensors: An Investigation using Artificial Neural Network

Mahdi Adabi[1], Reza Saber[1,2], Majid Naghibzadeh[3], Farnoush Faridbod[4], Reza Faridi-Majidi[1,2]*

[1] Department of Medical Nanotechnology, School of Advanced Technologies in Medicine, Tehran University of Medical Sciences, Tehran, Iran

[2] Research Center for Science and Technology in Medicine (RCSTIM), Tehran University of Medical Sciences, Tehran, Iran.

[3] Department of Nanotechnology, Research and Clinical Center for Infertility, Shahid Sadoughi University of Medical Sciences, Yazd, Iran

[4] Center of Excellence in Electrochemistry, Faculty of Chemistry, University of Tehran, Tehran, Iran

Corresponding author: Reza Faridi-Majidi

Tel: +98 (21) 88991118, Fax: +98 (21) 88991117

E-mail address: refaridi@tums.ac.ir

Abstract

The aim of this work was to investigate the effective parameters for predicting of the cathodic current in the polyacrylonitrile-based carbon nanofibers (CNFs) electrode using artificial neural network (ANN) method. The various factors including CNFs diameter, CNFs layer thickness, electrodeposition time of Pt on CNFs electrode, and solution pH of a phosphate buffer solution (PBS) containing $K_3Fe(CN)_6$ was designed to investigate the cathodic current of CNFs electrode. The different samples of the electrodes were fabricated as training and testing data-sets for ANN modeling. The best network had one hidden layer with 10 nodes in the layer. The mean squared error (MSE) and linear regression (R) between the observed and predicted cathodic current were 0.0763 and 0.9563, respectively, confirming the performance of the ANN. The obtained results using cyclic voltammetry (CV) exhibited that the cathodic current improves with decreasing the CNFs diameter, CNFs layer thickness, electrodeposition time of Pt on CNFs electrode and solution pH.

Keywords: Carbon nanofiber, electrode, polyacrylonitrile, electrochemical sensor, artificial neural network

Introduction

The working electrode plays a vital role for the electrochemical sensors and biosensors due to interface between electron transfer and solution. To date, different electrodes have been used in the electrochemical sensors and biosensors such as gold[1], platinum[2] and carbon paste electrode[3]. However, these metal electrodes have disadvantages such as formation of oxide layers or dissolution of metals and the limitation for using these electrodes in electroanalytical methods due to rather low hydrogen overvoltage[4], resulting in a decrease in analytical signals. In addition, Using oil in carbon paste electrode leads to decrease in the conductivity of electrodes[5]. Therefore, the synthesis of an efficient electrode with high electrical conductivity has attracted great attention in the electrochemical sensors and biosensors.

In recent years, with the development of nanotechnology, miniaturizing electrodes to nanoscale have received great attention. For example, gold nanorods were used on the gold electrode for the immobilization of single-stranded DNA because of high surface area to enhance the DNA biosensor performance[6]. Besides, carbon-based nanomaterials due to conductivity, high surface area, low background current, and functionality and wide potential window are candidates for constructing electrodes[7-9]. For example, carbon nanotubes have been used for modifying electrode due to increase in the surface area and facilitation in electron transfer reactions[10]. Among carbon-based nanomaterials, electrospun CNFs have attracted great interest due to unnecessary of binder, leads to increase in the conductivity[11]. They can be simultaneously used both for transducers and for matrixes[12]. CNFs were directly used as electrode without adding any binder and their results indicated good cyclic voltammetric response[13].

Electrospinning is composed of a high voltage power source, a nozzle and a collector. The potential difference between nozzle and collector results in the stretch of polymeric solution in form of thin jet from the nozzle toward the collector. In the stretch of polymeric solution process, the solvent evaporation occurs and solid nanofibers are collected on the collector[14-16]. Among the various precursors such as pitch and rayon for creating electrospun CNFs, polyacrylonitrile (PAN) is a high-performance polymer because of high carbon yield[17, 18].

Artificial neural networks (ANNs) have been recently applied to design the smart systems for investigating multi-variable complex processes and model the relationship between input variables and outputs[19-21]. ANNs take the inputs and create an output based on the associated weights of inputs using computation of the weighted sum of all inputs[22]. ANNs modeling begins by designing a network, training and testing process. After learning ANN via training dataset, the network is tested using test dataset[21] and finally the results are reported by an output layer.

The purpose of this work is to use ANN to identify the effective factors on the conductivity of CNFs electrodes, thus providing an insight into the preparation of CNFs electrodes for application in electrochemical sensors.

Materials and methods

Materials

The PAN with a molecular weight of 150,000 $g \cdot mol^{-1}$ was bought from Polyacryl Company (Iran). Potassium ferricyanide and Dimethylformamide (DMF) received from Merck Company. Na_2HPO_4 and KH_2PO_4 were purchased from Sigma-Aldrich Company. Phosphate buffer solution (PBS) was prepared by 0.1 M Na_2HPO_4 and 0.1 M KH_2PO_4. All solutions were prepared using ultra-pure water.

Preparation of Pt/CNF electrode

The CNF was prepared according to our previous work[13]. Briefly, the homogenous solutions were prepared by dissolving the PAN polymer in DMF. Electrospinning process was performed by Electroris (Fanavaran Nano Meghyas Ltd., Co., Tehran, Iran). A syringe pump with a feeding rate of 1.00 ml/h was applied to inject PAN solution from a plastic syringe towards the18-gauge needle and a high-voltage power supply was used to eject PAN solution from the spinneret toward a rotating collector under a voltage of 20 kV. The rotating drum and the distance between the needle and rotating collector covered with aluminum foil were 200 rpm and 10 cm, respectively. CNFs were then formed by stabilizing electrospun PAN nanofibers in an air atmosphere at 290 °C for 4 h with heating rate 1.5 °C min^{-1} and carbonizing the stabilized PAN nanofibers at 1000 °C for 1 h in an inert atmosphere with heating rate of 4 °C min^{-1} in a tube furnace, respectively. Afterwards, the CNF electrodes were prepared by spherically cutting the CNFs in size of 5 mm and inserting CNFs with a copper wire for the electrical contact. Then, CNFs electrode was immersed into 0.1 M HCl containing 10 mM H_2PtCl_6 and the electrodeposition was performed by potential -0.25 V. The current of corresponding electrodes was recorded by CV with scan number of 20 and scan rate of 100 $mV \cdot s^{-1}$ in the different pH.

Four ANN inputs include CNFs diameter (nm), CNFs thickness (micron), electrodeposition time of Pt on the CNF electrode (s) and pH of 5 mM $K_3Fe(CN)_6$ in 0.1 M PBS.

Artificial Neural Network

The predictive networks were examined with different hidden layers, and nodes, epochs and learning function. The validation of ANN models was investigated for predicting cathodic current of CNF/Pt electrodes by MATLAB software. The software employs neural networks for modeling the non-linear and complex relations between inputs and outputs and the response surfaces are shown via 3D graphs. In this work, the output is current of CNF electrodes, and the

inputs comprise of 4 variables, including PH, CNF diameter, CNF thickness, electrodeposition time of Pt on the CNF electrode. After investigating the plans using training and testing dataset, the best network with the highest accuracy and the lowest error was considered as an ANN model (a model with four inputs, one hidden layer with 10 nodes and one output layer). The best ANN algorithm was Levenberg-Marquardt back propagation. The transfer function in hidden layer and output layer of proposed network was log-sigmoid and purelin, respectively. The number of epochs between showing the progress, learning rate, momentum constant and maximum number of epochs to train was equal to 50, 0.01, 0.9, 100, respectively (the details are available in table 3).

Design of Network Models for predicting

The research was performed to predict the cathodic current using CV. Several parameters affect the current of corresponding electrodes including CNFs diameter, CNFs thickness, electrodeposition time of Pt and solution pH which measure cyclic voltammetric behavior of CNF electrode.

This study was performed to predict cathodic current of CNF electrodes. In order to detect relations among the parameters and their effects on cathodic current, ANN seems to be appropriate software to detect relations among the parameters and to find their impacts on the cathodic current. Different settings of four principal parameters on the cathodic current include CNFs diameter, CNFs thickness, electrodeposition time of Pt and solution pH. The Data as partition pairs (as shown in table 1) were classified in two groups: Training data (which regulate network values) and testing data (which was used for the validation and assessing network efficiency). The data were classified by the k-fold cross-validation method. As the small or large database is intersected by simple training-test, the performance or reliability of ANN will

decrease. Therefore, the method of k-fold cross-validation is used as statistically convincing conclusions which is more reliable than conventional training and testing dataset. In this technique, database is divided arbitrary into the equal k-subsets, including testing and training set.

After designing an ANN, and teaching the designed network via training dataset, the separate samples as testing dataset are used for validation, via calculating mean square error (MSE) and regression (R) (as shown in table 4). Therefore, each function of estimation approach repeated k times to fit function using training and testing process, separately.

The selected range of the variables is in the following:

(a) The selected range for pH in two levels of low and high was equal to 5 and 7, respectively.

(b) The selected range for CNFs layer thickness in two levels of low and high was equal to 100 and 200 nm, respectively.

(c) The selected range for the electrodeposition time of Pt on CNFs electrode in two levels of low and high was equal to 300 and 500 seconds, respectively.

(d) The selected range for CNFs diameter in two levels of low and high was equal to 76 and 110 nm, respectively.

The data were divided to the training and testing categories which adjust the network weights and investigate the network performance, respectively. Using k fold cross-validation method in comparison with training-test dataset dividing process results in less bias[23]. Therefore, the samples were randomly oriented on the 4 fold using a random numbers table. As shown in table 1, database was randomly partitioned into the k equal subsets and approximation function was repeated k times. At each step, a training set was created by placing k-1 subsets, and the

remaining k subsets are used as the test set. The mean squared error (MSE) of all test sets is calculated and referred to investigate the network validity.

Table 1

Table 2

Before using ANN technique, data normalization was carried out by equation (1):

$y_{norm} = (y_{max} - y_{min})(x - x_{min})/(x_{max} - x_{min}) + y_{min}$ (1)

In equation (1) y_{min} and y_{max} are -1 and 1 respectively. The x is the data which is normalized. x_{max} and x_{min} are the maximum and minimum values of x. Table 3 demonstrates the training parameters for ANN models.

Table 3

Results and discussion

The MSE and correlation coefficient (R) of the test data set obtained from ANN model including one hidden layer with 10 nodes are available in table 4.

Table 4

Mean square prediction error (MSPE) is given by the following equation (2):

$$MSPEn = \frac{100}{Nte\sigma_{dn}^{2}} \sum_{i=1}^{Nte} (d_n(i) - d_{pn}(i))^2, n = 1,...,5$$

Where d_n and d_{pn} are observed and predicted the cathodic current in n network, respectively. σ_{dn}^2 is the is the dn variance and Nte are the numbers of samples.

A linear regression was calculated to determine the correlation between the observed and predicted cathodic current (as shown in Fig. 1).

Fig. 1

The Pearson correlation coefficient between observed and predicted cathodic current was achieved equal to 0.942 which is significant at less than 0.01 % level (as seen in table 5).

Table 5

The Pearson correlation coefficients (r) between the observed (d_n) and predicted (d_{pn}) current is given by using equation (3):

$$r = \frac{n(\sum d_n d_{pn}) - (\sum d_n)(\sum d_{pn})}{\sqrt{[n(\sum {d_n}^2) - (\sum d_n)^2][n\sum {d_{pn}}^2) - (\sum d_{pn})^2]}}$$

where *n* is data number.

3D Plots of Current Predicted Patterns

In order to determine the effects of various parameters including CNFs diameter, CNFs thickness, electrodeposition time of Pt and pH on the cathodic current, 3D Plots are exhibited at the defined levels (as seen in Fig. 2-7).

As shown in Fig. 2, the most cathodic current in CV is approximately -85 μA in low diameter-low thickness level (Low D-Low Th). On the other hand, the least cathodic current is about -59 μA in high diameter-high thickness level (high D-high Th). The results indicated an inverse relationship between the cathodic current and CNFs diameter and CNFs layer thickness. In other word, decreasing diameter and layer thickness results in an increase in the cathodic current which is clear in all 3D plots. It can be attributed to better conductivity of CNFs as the diameter and thickness of CNFs decreased. The reason of increase in conductivity of CNFs electrode owing to decrease in CNFs diameter may be attributed to larger surface area[13].

Fig. 2

As seen in Fig. 3, the most and least cathodic current in CV is -83 and -64 μA which is related to the low electrodeposition time of Pt on CNFs- low CNFs diameter (low T-low D) and high electrodeposition time of Pt on CNFs- high CNFs diameter (high T-high D), respectively. The

results demonstrate that there is an inverse relationship between cathodic current and electrodeposition time of Pt on CNFs and CNFs diameter. The plots exhibit that improving peak in cathodic current occur as the electrodeposition time of Pt on CNFs and CNFs diameter decrease which is obvious in all 3D plots. The reason of the improvement in cathodic current because of the increase in electrodeposition time of Pt on CNFs may be related to surface area[24]. Because, decrease in electrodeposition time of Pt on CNFs results in the deposition of low amounts of Pt on CNFs electrode and consequently the increase in surface area.

Fig. 3

Based on the results in Fig. 4, the most cathodic current is equal to -82 μA which is related to low CNFs diameter-Low pH solution of $K_3Fe(CN)_6$ on low diameter-low pH (low D-low pH) and the least cathodic current is about -62 μA which belongs to high CNFs diameter-high pH solution of $K_3Fe(CN)_6$ in PBS (high D-high pH). The results indicate that there are an inverse relationship between the cathodic current and CNFs diameter and solution pH. The plots exhibit that by decreasing CNFs diameter and solution pH, the cathodic current progress. These results are observed in all 3D plots which is in agreement with the findings of M.M. Radhi et al.[25]. These results can be attributed to the H^+ ion which may activate the electrode surface and increase its response sensitivity[26].

Fig. 4

The minimum cathodic (about -63 μA) was seen in the high CNFs thickness- high electrodeposition time of Pt on CNFs (high Th-high T) (Fig. 5). In contrast, the maximum cathodic current (about -82 μA) was in the low CNFs thickness- low electrodeposition time of Pt on CNFs (low Th-low T). The results indicated that the cathodic current can improve as the CNFs thickness and the electrodeposition time of Pt on CNFs decrease. The reason of increase in

cathodic current due to decrease in CNFs thickness may be attributed to porosity. It means that with increasing the CNFs thickness, the CNFs were attached and packed to each other, resulting in a decrease in the porosity of CNFs electrodes and consequent decrease in the electrical conductivity of CNFs electrodes.

Fig. 5

As shown in Fig. 6, the least cathodic current and the most cathodic current are reported in -63 and -86 μA which belong to high CNFs thickness-high pH solution (high Th-high pH) and low CNFs thickness- low solution pH (low Th- low pH), respectively. The results exhibit that an inversely correlation between the cathodic current with CNFs thickness and solution pH. It means that by decreasing CNFs thickness and pH solution, the cathodic current improves.

Fig. 6

As seen in Fig. 7, the most cathodic current is equal to -82 μA which belong to low pH-low electrodeposition time of Pt on CNFs (low pH-low T) and the least cathodic current is about -66 μA which is related to high pH-high electrodeposition time of Pt on CNFs (high pH-high T). The results indicate that there is an inverse relationship between the cathodic current with electrodeposition time of Pt on CNFs and solution pH. The plots exhibit that by decreasing electrodeposition time of Pt on CNFs and pH solution, the cathodic current improves.

Fig. 7

Conclusion

This is the first report from effective parameters of for predicting cathodic current in CNFs electrode. The work showed the capability of ANNs to identify the factors affecting the cathodic current of CNFs electrode. In addition, 3D graphs developed from the model indicated that the preparation of CNFs electrodes plays a key role in the cathodic current. By decreasing CNFs

diameter, layer thickness and electrodeposition time of Pt on CNFs electrode, the cathodic current improved. It was also found that the solution pH of PBS containing $K_3Fe(CN)_6$ affects the cathodic current of CNF/Pt. It is suggested that the cathodic current is investigated using the electrodeposition of the other nanoparticles such as gold, palladium and copper on CNFs electrode. In addition, the investigation of other parameters affecting cathodic current such as porosity and surface area can be useful for the fabrication of CNF electrodes with more quality.

Acknowledgment

This project was supported by Tehran University of Medical Sciences (TUMS), grant No. 92-01-87-22097.

References

1. W. Cheng, W. Zhang, Y. Yan, B. Shen, D. Zhu, P. Lei and S. Ding, *Biosensors and Bioelectronics*, 2014, **62**, 274-279.
2. A. Jiménez, M. P. G. Armada, J. Losada, C. Villena, B. Alonso and C. M. Casado, *Sensors and Actuators B: Chemical*, 2014, **190**, 111-119.
3. H. Karimi-Maleh, A. L. Sanati, V. K. Gupta, M. Yoosefian, M. Asif and A. Bahari, *Sensors and Actuators B: Chemical*, 2014, **204**, 647-654.
4. B. Uslu and S. A. Ozkan, *Combinatorial chemistry & high throughput screening*, 2007, **10**, 495-513.
5. N. T. Xuyen, E. J. Ra, H.-Z. Geng, K. K. Kim, K. H. An and Y. H. Lee, *The Journal of Physical Chemistry B*, 2007, **111**, 11350-11353.
6. Z. Shakoori, S. Salimian, S. Kharrazi, M. Adabi and R. Saber, *Analytical and bioanalytical chemistry*, 2015, **407**, 455-461.
7. F. Marken, M. L. Gerrard, I. M. Mellor, R. J. Mortimer, C. E. Madden, S. Fletcher, K. Holt, J. S. Foord, R. H. Dahm and F. Page, *Electrochemistry communications*, 2001, **3**, 177-180.
8. M. E. Ghica, R. Pauliukaite, O. Fatibello-Filho and C. M. A. Brett, *Sensors and Actuators B: Chemical*, 2009, **142**, 308-315.
9. C. Xiang, Y. Zou, L.-X. Sun and F. Xu, *Electrochemistry communications*, 2008, **10**, 38-41.
10. M. Adabi, R. Saber, M. Adabi and S. Sarkar, *Microchimica Acta*, 2011, **172**, 83-88.
11. C. Kim, S.-H. Park, W.-J. Lee and K.-S. Yang, *Electrochimica Acta*, 2004, **50**, 877-881.
12. A. Arvinte, F. Valentini, A. Radoi, F. Arduini, E. Tamburri, L. Rotariu, G. Palleschi and C. Bala, *Electroanalysis*, 2007, **19**, 1455-1459.
13. M. Adabi, R. Saber, R. Faridi-Majidi and F. Faridbod, *Materials Science and Engineering: C*, 2015, **48**, 673-678.
14. R. Faridi-Majidi and N. Sharifi-Sanjani, *Journal of applied polymer science*, 2007, **105**, 1351-1355.
15. N. Bhardwaj and S. C. Kundu, *Biotechnology advances*, 2010, **28**, 325-347.
16. S. S. Esnaashari, S. Rezaei, E. Mirzaei, H. Afshari, S. M. Rezayat and R. Faridi-Majidi, *International journal of biological macromolecules*, 2014, **70**, 50-56.
17. S. K. Nataraj, K. S. Yang and T. M. Aminabhavi, *Progress in polymer science*, 2012, **37**, 487-513.
18. X. Huang, *Materials*, 2009, **2**, 2369-2403.
19. J. Bourquin, H. Schmidli, P. van Hoogevest and H. Leuenberger, *European journal of pharmaceutical sciences*, 1998, **6**, 287-300.
20. P. M. Sathe and J. Venitz, *Drug development and industrial pharmacy*, 2003, **29**, 349-355.
21. M. Naghibzadeh and M. Adabi, *Fibers and Polymers*, 2014, **15**, 767-777.
22. A. Amani, P. York, H. Chrystyn and B. J. Clark, *Pharmaceutical research*, 2010, **27**, 37-45.
23. R. Kohavi, *Lawrence Erlbaum Associates Ltd*, **14**, 1137-1145.
24. X. Chu, D. Duan, G. Shen and R. Yu, *Talanta*, 2007, **71**, 2040-2047.
25. M. M. Radhi, E. A. J. Al-Mulla and W. T. Tan, *Research on Chemical Intermediates*, 2014, **40**, 179-192.
26. J. Wu, J. Zhu, L. Shan and N. Cheng, *Analytica chimica acta*, 1996, **333**, 125-130.

Table captions:

Table 1. Training-testing partition pairs using 4-fold cross-validation method

Table 2. Training data set for ANNs

Table 3. ANN training parameters

Table 4. MSE and R of 4-fold test data in the selected ANN network

Table 5. Pearson correlation between the observed and predicted current of CNF electrode.

Figure captions:

Fig. 1. Regression plot between the observed and predicted current.

Fig. 2. The data and 3D plots of cathodic current of CNFs electrode (Z axis) predicted by ANN fixed at mentioned levels (CNFs diameter=D and CNFs thickness=Th).

Fig. 3. The data and 3D plots of cathodic current of CNFs electrode (Z axis) predicted by ANN fixed at mentioned levels (CNFs diameter=D and electrodeposition time of Pt on the CNF electrode=T).

Fig. 4. The data and 3D plots of cathodic current of CNFs electrode (Z axis) predicted by ANN fixed at mentioned levels (CNFs diameter=D and pH).

Fig. 5. The data and 3D plots of cathodic current of CNFs electrode (Z axis) predicted by ANN fixed at mentioned levels (CNFs thickness=Th and electrodeposition time of Pt on the CNF electrode=T).

Fig. 6. The data and 3D plots of cathodic current of CNFs electrode (Z axis) predicted by ANN fixed at mentioned levels (CNFs thickness=Th and pH).

Fig. 7. The data and 3D plots of cathodic current of CNFs electrode (Z axis) predicted by ANN fixed at mentioned levels (pH and electrodeposition time of Pt on the CNF electrode=T).

Table 1. Training-testing partition pairs using 4-fold cross-validation method

Partition pairs	Training set	Testing set
1	**Partition {1,2,3,}**	Partition {4}
2	**Partition {1,2,4}**	Partition {3}
3	**Partition {1,3,4}**	Partition {2}
4	**Partition {2,3,4}**	Partition {1}

Table 2. Training data set for ANNs

Sample	Nanofibers diameter (nm)	Thickness (micron)	Electrodeposition time of Pt (sec)	pH	Observed current (μA)	Predicted current (μA)
1	110	100	500	5	-76. 24	-76.74
2	76	100	500	5	-90.05	-83.74
3	110	200	300	5	-60.70	-72.38
4	110	100	300	5	-88.04	-90.05
5	110	100	500	7	-65.66	-61.79
6	76	200	300	5	-87.94	-85.80
7	110	200	500	7	-57.09	-57.09
8	110	200	500	5	-59.72	-59.72
9	76	200	500	5	-70.41	-70.31
10	76	100	500	7	-76.18	-76.18
11	76	200	300	7	-69.63	-65.72
12	76	100	300	7	-83.36	-87.94
13	76	100	300	5	-92.70	-92.70
14	76	200	500	7	-65.72	-68.88
15	110	200	300	7	-58.83	-58.83
16	110	100	300	7	-67.52	-70.02

Table. 3 ANN training parameters

Algorithm= trainlm
(Levenberg-Marquardt back propagation)
Transfer function in hidden layers=log-sigmoid and purelin
Number of epochs between showing the progress = 50
Learning rate = 0.01
Momentum constant = 0.9
Maximum number of epochs to train = 100;
Performance goal= 1e-5;

Table 4. MSE and R of 4-fold test data in the selected ANN network

Data set	Test MSE	Test R
1	0.05	0.9648
2	0.0497	0.9714
3	0.0351	0.97045
4	0.1702	0.92037
Mean	0.0763±0.06302	0.9563±0.02443

Table 5. Pearson correlation between the observed and predicted current of CNF electrode

		predicted currents(μA)	observed currents (μA)
predicted currents(μA)	Pearson Correlation	1	.942**
	Sig. (2-tailed)		.000
	N	16	16
observed currents (μA)	Pearson Correlation	.942**	1
	Sig. (2-tailed)	.000	
	N	16	16

**. Correlation is significant at the 0.01 level (2-tailed).

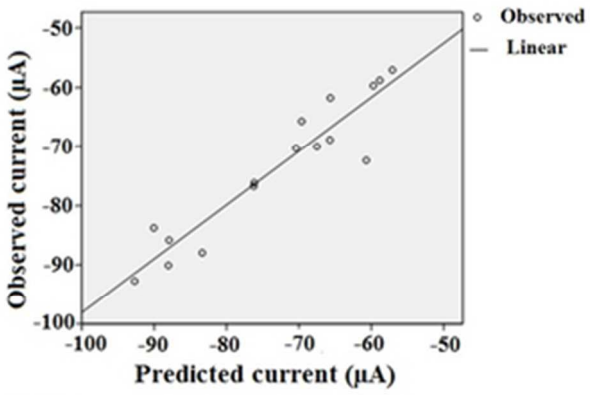

Fig. 1

Regression plot between the observed and predicted current
25x18mm (300 x 300 DPI)

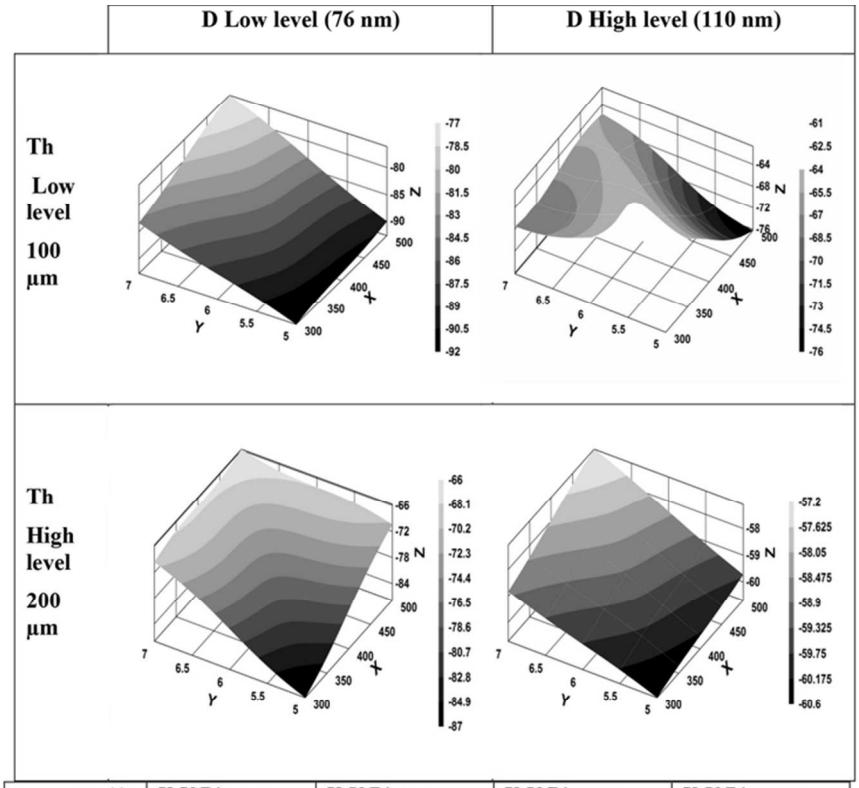

current (µA) (Z)	X-Y Diagram Low D-Low Th	X-Y Diagram High D -Low Th	X-Y Diagram Low D- High Th	X-Y Diagram High D- High Th
Minimum Z	-92.7 µA at X = 300, Y = 5	-76.24 µA at X = 500, Y = 5	-87.94 µA at X = 300, Y = 5	-60.7 µA at X = 300, Y = 5
Maximum Z	-76.18 µA at X = 500, Y = 7	-60.7 µA at X = 300, Y = 5	-65.72 µA at X = 500, Y = 7	-57.09 µA at X = 500, Y = 7
Mean	-85.5725 µA	-67.53 µA	-73.425 µA	-59.085 µA
STD	7.392868	6.480998	9.891823	1.533677

X= Time (s), Y= pH, Z= Current (µA), D= Nanofibers diameter (nm), Th= nanofibers layer thickness (µm)

Fig.2

The data and 3D plots of cathodic current of CNFs electrode (Z axis) predicted by ANN fixed at mentioned levels (CNFs diameter=D and CNFs thickness=Th)
72x78mm (300 x 300 DPI)

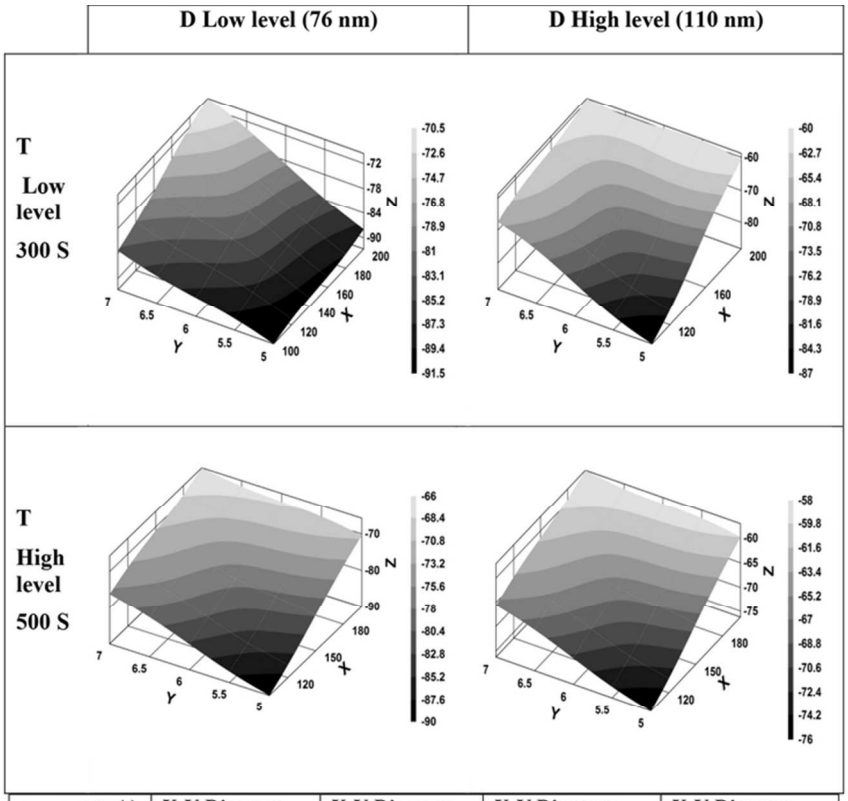

current (µA) (Z)	X-Y Diagram Low D-Low T	X-Y Diagram High D -Low T	X-Y Diagram Low D- High T	X-Y Diagram High D- High T
Minimum Z	-92.7 µA at X = 100, Y = 5	-88.04 µA at X = 100, Y = 5	-90.05 µA at X = 100, Y = 5	-76.24 µA at X = 100, Y = 5
Maximum Z	-69.63 µA at X = 200, Y = 7	-58.83 µA at X = 200, Y = 7	-65.72 µA at X = 200, Y = 7	-57.09 µA at X = 200, Y = 7
Mean	-83.4075 µA	-68.7725 µA	-75.59 µA	-64.695 µA
STD	9.945	13.377	10.546	8.487

X= Nanofibers layer thickness (µm), Y= pH, Z= Current (µA), D= Nanofibers diameter (nm), T= Time (s)

Fig.3

The data and 3D plots of cathodic current of CNFs electrode (Z axis) predicted by ANN fixed at mentioned levels (CNFs diameter=D and electrodeposition time of Pt on the CNF electrode=T)
73x80mm (300 x 300 DPI)

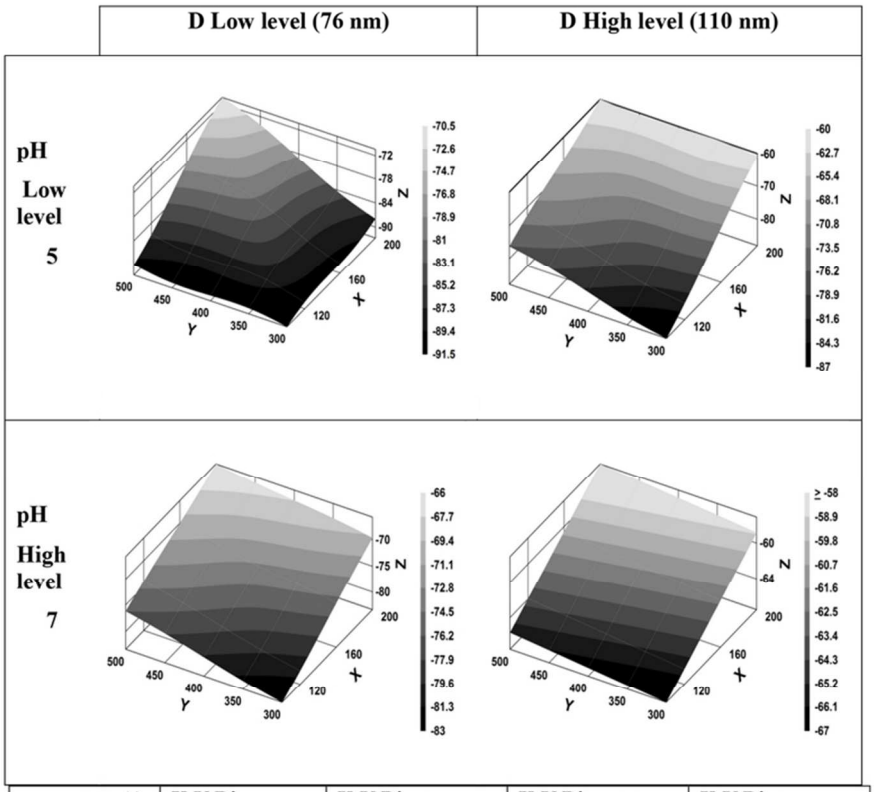

current (µA) (Z)	X-Y Diagram Low D-Low pH	X-Y Diagram High D -Low pH	X-Y Diagram Low D- High pH	X-Y Diagram High D- High pH
Minimum Z	-92.7 µA at X = 100, Y = 300	-88.04 µA at X = 100, Y = 300	-83.36 µA at X = 100, Y = 300	-62.52 µA at X = 100, Y = 300
Maximum Z	-70.41 µA at X = 200, Y = 500	-59.72 µA at X = 200, Y = 500	-65.72 µA at X = 200, Y = 500	-57.09 µA at X = 200, Y = 500
Mean	-82.275 µA	-71.175 µA	-73.722 µA	-62.275 µA
STD	10.1	13.55	7.74	5.09

X= Nanofibers layer thickness (µm), Y= Time (s), Z= Current (µA), D= Nanofibers diameter (nm)

Fig.4

The data and 3D plots of cathodic current of CNFs electrode (Z axis) predicted by ANN fixed at mentioned levels (CNFs diameter=D and pH)
75x87mm (300 x 300 DPI)

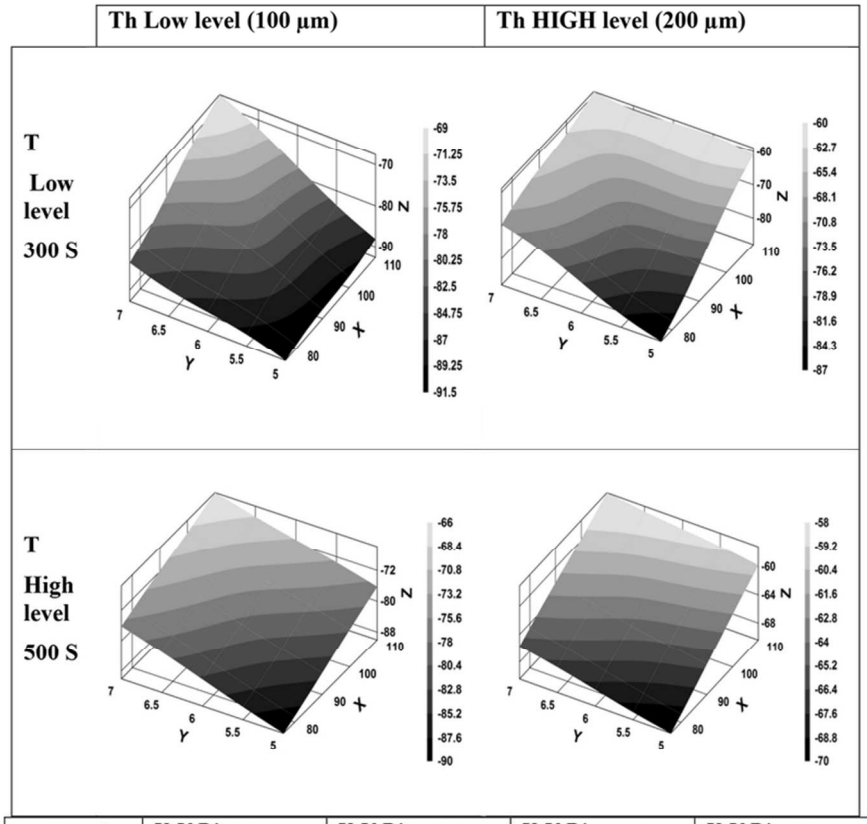

current (µA) (Z)	X-Y Diagram Low TH-Low T	X-Y Diagram High TH -Low T	X-Y Diagram Low TH- High T	X-Y Diagram High TH- High T
Minimum Z	-92.7 µA at X = 76, Y = 5	-87.94 µA at X = 76, Y = 5	-90.05 µA at X = 76, Y = 5	-70.41 µA at X = 76, Y = 5
Maximum Z	-67.52 µA at X = 110, Y = 7	-58.83 µA at X = 110, Y = 7	-65.66 µA at X = 110, Y = 7	-57.09 µA at X = 110, Y = 7
Mean	-82.905µA	-69.275 µA	-77.0325 µA	-63.2525 µA
STD	10.94	13.31	10	5.98

X= Nanofibers diameter (nm), Y= pH, Z= Current (µA), TH= Nanofibers layer thickness (µm),T=Time (s)

Fig.5

The data and 3D plots of cathodic current of CNFs electrode (Z axis) predicted by ANN fixed at mentioned levels (CNFs thickness=Th and electrodeposition time of Pt on the CNF electrode=T)
77x93mm (300 x 300 DPI)

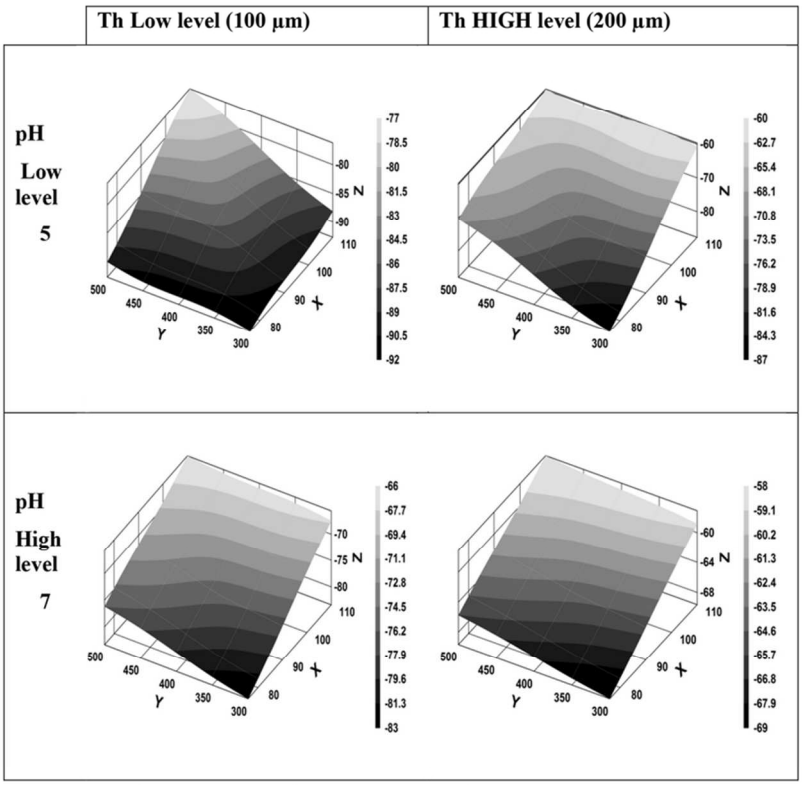

current (µA) (Z)	X-Y Diagram Low TH-Low pH	X-Y Diagram High TH -Low pH	X-Y Diagram Low TH- High pH	X-Y Diagram High TH- High pH
Minimum Z	-92.7 µA at X = 76, Y = 300	-87.94 µA at X = 76, Y = 300	-83.36 µA at X = 76, Y = 300	-69.63 µA at X = 76, Y = 300
Maximum Z	-76.24 µA at X = 110, Y = 500	-59.72 µA at X = 110, Y = 500	-65.66 µA at X = 110, Y = 500	-57.09 µA at X = 110, Y = 500
Mean	-86.7575 µA	-69.69 µA	-73.18 µA	-63.82 µA
STD	7.27	13.09	8.19	5.87

X= Nanofibers diameter (nm), Y= Time (s), Z= Current (µA), TH= Nanofibers layer thickness (µm),

Fig.6

The data and 3D plots of cathodic current of CNFs electrode (Z axis) predicted by ANN fixed at mentioned levels (CNFs thickness=Th and pH)
83x102mm (300 x 300 DPI)

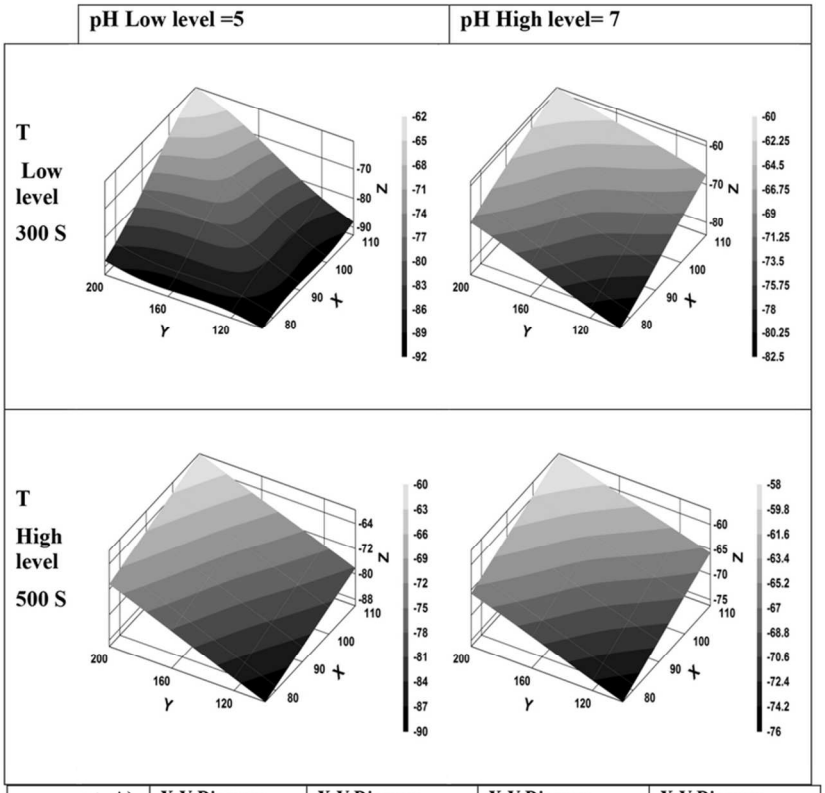

current (μA) (Z)	X-Y Diagram Low pH- Low T	X-Y Diagram High pH -Low T	X-Y Diagram Low pH- High T	X-Y Diagram High pH- High T
Minimum Z	-92.7 μA at X = 76, Y = 100	-83.36 μA at X = 76, Y = 100	-90.05 μA at X = 76, Y = 100	-76.18 μA at X = 76, Y = 100
Maximum Z	-60.7 μA at X = 110, Y = 200	-58.83 μA at X = 110, Y = 200	-59.72 μA at X = 110, Y = 200	-57.09 μA at X = 110, Y = 200
Mean	-82.345 μA	-69.83 μA	-74.105 μA	-66.16 μA
STD	14.59	10.15	12.64	7.81

X= Nanofibers diameter (nm), Y= Nanofibers layer thickness (μm),T= Time (s), Z= Current (μA)

Fig.7

The data and 3D plots of cathodic current of CNFs electrode (Z axis) predicted by ANN fixed at mentioned levels (pH and electrodeposition time of Pt on the CNF electrode=T)
82x104mm (300 x 300 DPI)